

# Identification of Ice Nucleation Active Sites on Feldspar Dust Particles

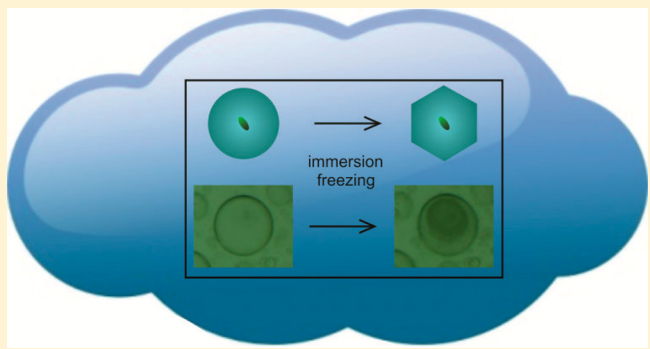
Tobias Zolles,<sup>†</sup> Julia Burkart,<sup>†,||</sup> Thomas Häusler,<sup>†</sup> Bernhard Pummer,<sup>†,⊥</sup> Regina Hitzenberger,<sup>‡</sup> and Hinrich Grothe\*,<sup>†</sup>

<sup>†</sup>Institute of Materials Chemistry, Vienna University of Technology, Getreidemarkt 9, 1060 Vienna, Austria

<sup>‡</sup>Faculty of Physics, Aerosol Physics and Environmental Physics, University of Vienna, Boltzmanng. 5, 1090 Vienna, Austria

## Supporting Information

**ABSTRACT:** Mineral dusts originating from Earth's crust are known to be important atmospheric ice nuclei. In agreement with earlier studies, feldspar was found as the most active of the tested natural mineral dusts. Here we investigated in closer detail the reasons for its activity and the difference in the activity of the different feldspars. Conclusions are drawn from scanning electron microscopy, X-ray powder diffraction, infrared spectroscopy, and oil-immersion freezing experiments. K-feldspar showed by far the highest ice nucleation activity. Finally, we give a potential explanation of this effect, finding alkali-metal ions having different hydration shells and thus an influence on the ice nucleation activity of feldspar surfaces.



## INTRODUCTION

The largest uncertainty in the influence of aerosol particles and clouds on the climate system is caused by aerosol–cloud interactions, which are not adequately represented in climate modeling.<sup>1</sup> Cloud microphysics determine cloud albedo in the visible and infrared (IR) spectral ranges, cloud lifetime, and precipitation properties.<sup>2</sup> Cloud radiative properties are strongly linked to the microphysical state of clouds such as number concentration and size of liquid droplets and ice crystals.<sup>2,3</sup> Aerosol particles can act as cloud condensation nuclei (CCN) and as ice nuclei (IN) influencing the aggregation state and the microphysical properties of cloud particles. Knowledge on the glaciation of clouds is essential to estimate cloud radiative forcing on the climate system.<sup>4,5</sup>

In the atmosphere ice crystals form through heterogeneous and homogeneous ice nucleation. At temperatures below 235 K homogeneous nucleation takes place, whereas at higher temperatures ice does not form spontaneously.<sup>6</sup> In this temperature range ice nucleation occurs heterogeneously; i.e., it is triggered by the presence of aerosol particles providing foreign surfaces that reduce the energy barrier for nucleation. Aerosol particles that can initiate the freezing process are termed IN.

Several mechanisms are known by which aerosol particles catalyze the formation of the ice phase in clouds: deposition, condensation, contact, and immersion freezing.<sup>6</sup> The deposition mode involves the growth of ice directly from the vapor phase, whereas condensation freezing occurs if the ice phase is formed immediately after condensation of water vapor on a solid particle as liquid intermediate. If an IN has already been immersed in a droplet and causes freezing, the process is termed immersion

freezing. Contact freezing happens if a supercooled droplet freezes at the moment of contact with an IN. In mixed-phase (liquid and ice) and cirrus clouds the dominant nucleation mechanism is suspected to be immersion or contact freezing, and to a lesser extent deposition nucleation.<sup>7</sup> The ice nucleating ability of an aerosol particle in each of the four modes at fixed temperature and humidity conditions depends on its physicochemical properties, e.g., surface structure, size, and/or chemical composition.

Although several requirements for an effective IN have already been proposed decades ago, the exact mechanisms of nucleation are still not adequately understood.<sup>6</sup> It is known that the ice nucleation efficiency of a particle is not necessarily determined by the entire particle but by so-called active sites on the particle's surface. However, information on the nature and location of active sites is still limited and a prediction of the ice nucleation efficiency of a particle based on its physicochemical properties is not yet possible.<sup>8,9</sup>

Mineral dusts have been known to act as IN for a long time.<sup>6,10,11</sup> Atmospheric mineral particles originate from arid regions such as deserts, from volcanic eruptions and from soil due to agricultural use. They are released into the air by the action of wind and are omnipresent in our atmosphere.<sup>12</sup>

Recent studies confirm the importance of mineral dust particles for ice cloud formation. Aerosol mass spectrometry

**Special Issue:** Markku Räsänen Festschrift

**Received:** September 29, 2014

**Revised:** January 13, 2015

**Published:** January 13, 2015

suggested that 50% of the material in ice crystal residues in clouds over Wyoming was composed of mineral dusts.<sup>13</sup> Another *in situ* study analyzed the residual particles within cirrus ice crystals and found an enrichment of mineral dust particles of 61% compared to their near-cloud abundance.<sup>14</sup>

Natural dust particles rarely consist of pure mineral phases but are internal mixtures of diverse mineral components covered with other inorganic, organic, and/or biological substances. The main mineral dust particles found in the atmosphere are clays (kaolinite, illite, montmorillonite), quartz, feldspars, and calcite.

Within the last years, extensive efforts have been made to better understand and predict the role of mineral dusts in the formation of atmospheric ice clouds. Several laboratory studies on the ice nucleation activity (INA) of mineral dust particles have been performed by many groups. Because different measurement techniques are applied, the comparison of the results is often challenging.<sup>5</sup> An extensive comparison and overview of the studies on mineral dusts was given in recent years.<sup>8,9</sup>

Most studies focused on clay minerals with kaolinite being the clay mineral studied most intensively.<sup>15–18</sup> In all studies kaolinite shows INA in immersion freezing mode above 243 K. In a study of all common clay materials using the same method, illite was found to be the most active IN followed by kaolinite and montmorillonite.<sup>17</sup>

The study by Zimmermann et al.<sup>19</sup> gives a good comparison between the INA of different minerals in the deposition mode. The INA of closely related materials, like the feldspars, was rather different. In fact, microcline (K-feldspar) needed the lowest supersaturation at 261 K to initiate ice formation (i.e., IN activation). The species active at the lowest supersaturation were kaolinite, illite, hematite, and microcline. Kaolinite and hematite activated at quite high temperatures. Another comparative study was performed in the deposition mode.<sup>20</sup> Kaolinite and muscovite were found to be active at lower supersaturations and were therefore considered rather efficient IN, whereas quartz and calcite were poor IN. Montmorillonite was found a good IN below a temperature around 241 K.

Most of the laboratory studies on mineral dust either focused on clay minerals that are often obtained from natural samples or on purely natural dusts. Concerning natural dusts, Arizona Test Dust (ATD) is the most widely used proxy within the field. Initial freezing is reported around 249 K.<sup>21</sup> Another natural dust sample frequently studied is volcanic ash.<sup>22,23</sup> Many of these natural dusts are mixtures of different clays, quartz, and feldspars with varying composition. Recently Atkinson et al.<sup>24</sup> performed the first comparative study on ice nucleation in the immersion mode looking not only at single minerals from the clay group but also at K-feldspar, Na/Ca-feldspar, quartz, and calcite as well. Almost simultaneously Yakobi-Hanock et al.<sup>25</sup> conducted a similar study on ice nucleation of 24 mineral samples in the deposition mode. Both studies find the ice nucleating ability of K-feldspar exceptionally high compared to other minerals. In the immersion mode K-feldspar already nucleates ice at temperatures of 250.5 K whereas for the other minerals only lower nucleation temperatures were found.<sup>24</sup> Only recently was the INA of K-feldspar found to be even better than that of Na/Ca-feldspar (247 K). Atkinson et al.<sup>24</sup> conclude that K-feldspar is the key component determining the INA of atmospheric mineral dusts.

As already mentioned, the majority of the studies concentrated on the experimental description of the ice nucleation behavior of mineral dusts. In case of immersion freezing initial and/or median freezing temperatures are reported for a vast set of atmospherically relevant minerals.<sup>8</sup> An explanation of the INA on

a molecular level is attempted only rarely.<sup>26,27</sup> One exception is the recent study by Yakobi-Hanock et al.<sup>25</sup> where the authors relate the INA of the different minerals to their particular surface charges. For example, they suggest that the IN properties of clays, especially of the ice active kaolinite, might be due to electrostatic interactions between their charged surfaces, counterions and the polar water molecule. Minerals with such ionic surfaces are believed to promote ice nucleation, as they are more likely to form hydrogen bonds with water molecules. Shen et al.<sup>28</sup> found fluorine mica as an example of extremely high INA. Apparently, the ice embryos are sustained on mica by F–H–O hydrogen bonds assisted by neighboring K<sup>+</sup> ions.

Overall, a fundamental understanding of the heterogeneous ice nucleation on mineral dusts is still missing. For example, the nature of active sites is a matter of speculation only.

The goal of our study was to investigate the INA of selected mineral particles as well as their chemical nature to identify possible characteristics of active sites. We performed experiments with the oil-immersion freezing method with pure and pretreated (heated, enzymatic pretreated, milled) dust particles. In addition, we characterized the particles with field emission gun scanning electron microscopy (FEG-SEM) and tunneling electron microscopy (TEM), energy-dispersive X-ray spectroscopy (EDX), X-ray powder diffraction (XRD), and attenuated total reflection Fourier transform infrared spectroscopy (ATR-FTIR). Combining these data we propose a possible explanation why specific minerals, in particular K-feldspars, are good IN, whereas others are not. On the basis of the experiments, we propose a first interpretation of the nature of active sites.

## ■ EXPERIMENTAL SECTION

Oil-immersion freezing experiments under a cryomicroscope were carried out to test the INA of different mineral dust samples. In addition, the particles were characterized regarding their surface and bulk properties by the following set-ups.

**Cryomicroscopy.** Nucleation properties of the samples were obtained with an optical microscope and a homemade cryocell. The experimental setup has already been used in former studies, and a detailed description can be found elsewhere.<sup>29</sup> Here, only a short description of the principle is given.

The core of the experiment is a thermoregulated cryocell consisting of a Peltier element in a Teflon box. The cryocell that has a glass window on top is placed on an Olympus BX51 optical microscope desk below the objective. Photos can be taken with a MDC-200 microscope camera.

The mineral dust samples were studied in the oil-immersion mode: a drop of an oil matrix (80–85 wt % paraffin, 15–20 wt % lanolin) with dispersed small water droplets (10–40 μm) containing mineral dust particles was put on a glass slide and placed on the Peltier stage. The Peltier element was then chilled at a constant cooling rate, until all visible droplets were frozen. In earlier measurements, no influence of the cooling rate (0.1–10 K/min) on the median freezing temperature was found within the uncertainty of the method, which is about ±1 K (see Supporting Information). Whenever freezing of droplets was observed, a picture was taken and the respective temperature was recorded. Frozen droplets can be easily distinguished from liquid ones as they appear dark due to increased light scattering and contain visible internal structures, such as edges or cubes.

Finally, each picture was analyzed to determine the fraction of frozen droplets, which was then plotted against temperature to obtain a nucleation curve characteristic for a specific sample. To compare different nucleation curves, we determined the median

Table 1. 13 Studied Minerals Listed Together with the Composition Determined with XRD and EDX as Far as Possible<sup>a</sup>

mineral	composition	source	particle size [μm]	$T_{50}$ [K]
quartz I	pure alpha quartz	Sigma-Aldrich	1–5 (80%)	249 ± 1
quartz II	pure alpha quartz	Fluka	1–5	240 ± 1
quartz III	pure alpha quartz	natural quartz	1–15	235 ± 0
K-feldspar/microcline	70–80% microcline, rest: albite	Alfa Aesar	1–10	249 ± 1
Na-feldspar/albite	>99% albite	Alfa Aesar	1–10	239 ± 1
Na/Ca-feldspar/andesine	anorthian andesine (Na:Ca 50:50)	Alfa Aesar	1–10	240 ± 1
montmorillonite	quartz, muscovite, montmorillonite (no quantification)	Sigma-Aldrich	0.5–10	240 ± 1
kaolinite	5–10% quartz, 5–10% muscovite, 5–10% halloysite, rest kaolinite	Bulus Alba	0.5–5	248 ± 1
calcite	>99% calcite	Sigma-Aldrich	2–5	237 ± 1
gypsum	96% $\text{CaSO}_4 \cdot 2\text{H}_2\text{O}$ , 4% $\text{CaSO}_4 \cdot \frac{1}{2}\text{H}_2\text{O}$	Sigma-Aldrich	needles: 5–15	239 ± 1
volcanic ash	feldspars (ca. 70% albite), quartz, iron–titanium oxide	ICE-SAR	1–50	238 ± 1
Arizona test dust	17% sodium andesine, 17% K-feldspar, 5–10% other feldspars, rest: quartz	PTI	1–10	250 ± 1
limestone	>99% calcite	natural sampled	1–20	237 ± 1

<sup>a</sup>The particle size was estimated from the SEM images. The  $T_{50}$  is listed for a particle concentration of 20 mg/mL.

freezing temperature,  $T_{50}$ , which is the temperature where 50% of all droplets in the picture are frozen. This value is more reliable than the initial freezing temperature, which is the temperature where the first droplet freezes, because the latter may be influenced by statistical variations and is less reproducible.

**Electron Microscopy.** SEM and TEM measurements were performed at the USTEM at the Vienna University of Technology. For SEM, the milled mineral dust samples were put on a graphite plate and coated with 4 nm of Au/Pd alloy by sputtering (program: 30 s, 15 mA). Images with 1000 $\times$ , 10000 $\times$ , and 20000 $\times$  magnifications were taken. The experiments were performed with an FEI Quanta 200 FEG-SEM. TEM pictures were taken with the FEI TECNAI F20. Both instruments also allow us to measure EDX spectra.

**X-ray Powder Diffraction.** In powder XRD, polycrystalline minerals with grain sizes around 1  $\mu\text{m}$  can be easily analyzed. The powder is placed on a steel sample holder and then inserted into an X-ray diffractometer (PanalyticalX'Pert pro; Bragg–Brentano geometry). The  $2\theta$  angle was varied between 5° and 120°. As X-ray source, the Cu  $\text{K}\alpha$  line was used in all the experiments (0.154 44 nm). All samples were used without further treatment prior to the XRD experiments except milling. The measuring time varied between 1 h for the single mineral samples and 3 h for the natural samples. The diffractograms were compared to diffractogram databases to obtain a semiquantitative phase analysis.<sup>30</sup>

**Infrared Spectroscopy.** ATR-FTIR measurements were performed on the mineral dust particles. The FTIR study of the mineral samples was taken on a Bruker Vector 22. Germanium was used as ATR-crystal. At least 1000 scans were collected per sample to get a sufficient signal-to-noise ratio at 4  $\text{cm}^{-1}$  spectral resolution.

**Nitrogen Adsorption.** The surface areas of the quartz and montmorillonite samples were measured using a commercial liquid nitrogen adsorption system (ASAP2020, Micromeritics). Data evaluation was based on the model by Brunauer, Emmett, and Teller (BET).<sup>31</sup> The surface areas of the other mineral dust samples could not be measured as too little material was available. The geometrical surface area of those minerals was estimated on the basis of the SEM images.

**Sample Description and Preparation.** In total the INA of 13 different mineral dust samples was investigated with the cryomicroscope. The studied samples are calcite, gypsum, three different quartz samples (quartz I, quartz II, quartz III), microcline, albite, andesine, Arizona Test Dust (ATD),

montmorillonite, kaolinite, limestone, and volcanic ash (Table 1).

The INA of the mineral dust particles was investigated with pure (as purchased) and freshly milled, heat-treated, and enzyme-treated particles. Three sets of experiments were performed with pretreated samples:

First, the minerals were milled to initial sizes between 1 and 10  $\mu\text{m}$  with an agate mortar or a swing mill (Retsch MM400). Suspensions of mineral dust particles in Milli-Q water with concentrations of 20 and 50 mg/mL were prepared and then mixed with oil to obtain an emulsion. The water droplets in the emulsion were 10–40  $\mu\text{m}$  in size and contained around 1–10 particles at a concentration of 20 mg/mL and about twice as much at concentrations of 50 mg/mL. The INA of all samples was determined.

Second, the most ice nucleation active samples were selected and heated at 523 K for 4–5 h. In addition, the feldspars and quartz I were also heated at 373 and 773 K to control for surface alteration with temperature and to remove possible organic impurities, which are known to promote ice nucleation in some cases, and to ensure that the INA is only related to the mineral phases.<sup>32</sup> For all temperature-treated particles the INA was determined before and after the heat treatment.

Third, selected samples were treated with enzymes to exclude the possibility that their INA is due to adsorbed biological impurities, and to specifically block nucleation sites.<sup>32</sup> For observing the impact of specific blocking, it was important to select a submolecular coverage of the mineral surface. Otherwise, the effect would not be related to the sites but would be due to the entire coverage only. As enzymes we used papain (2 mg/mL), pronase E (5 mg/mL), cellulose onozuka (5 mg/mL), and lipase (2 mg/mL), which break down proteins, polysaccharides, or lipids. Three different enzymatic treatment experiments were performed. After each step ice nucleation measurements were performed: (a) first, each enzyme was added to separate suspensions of pure Milli-Q water and mineral dust particles and left for 3–5 h at incubation temperatures of 308 K (lipase), 310 K (pronase E, onozuka) and 340 K (papain), (b) second, the enzymes were added all at once to the suspensions and the samples were left in incubation in total for 5 h increasing the temperature stepwise, respectively, and (c) in the last step, the enzymes were added and nucleation measurements were conducted immediately without incubation.

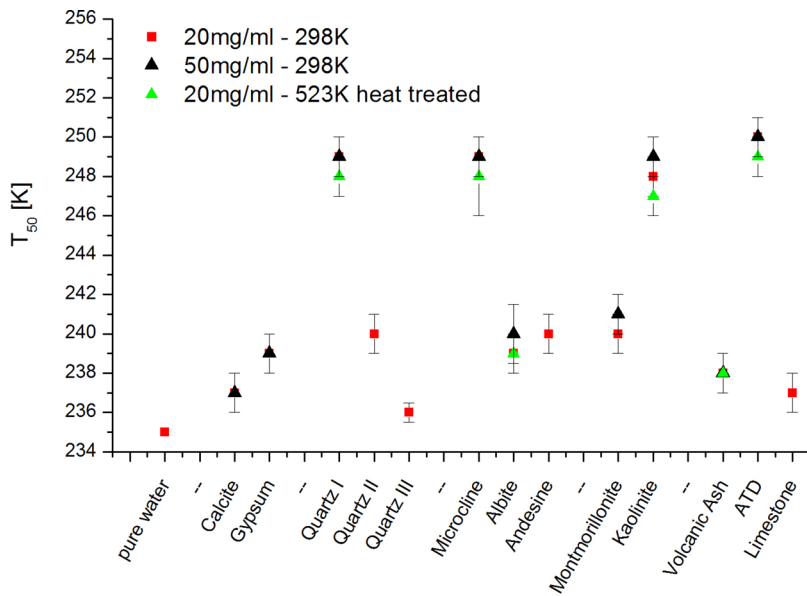


**Figure 1.** Median freezing temperatures ( $T_{50}$ ) for all minerals. The error bars are taken from the 33 and 66% freezing ratios. The minerals are grouped into nonsilicates, quartz, feldspar, clays, and natural samples. The most active dusts are quartz, microcline (K-feldspar), ATD, and kaolinite. The particle diameters were 1–10  $\mu\text{m}$  and are listed in Table 1.

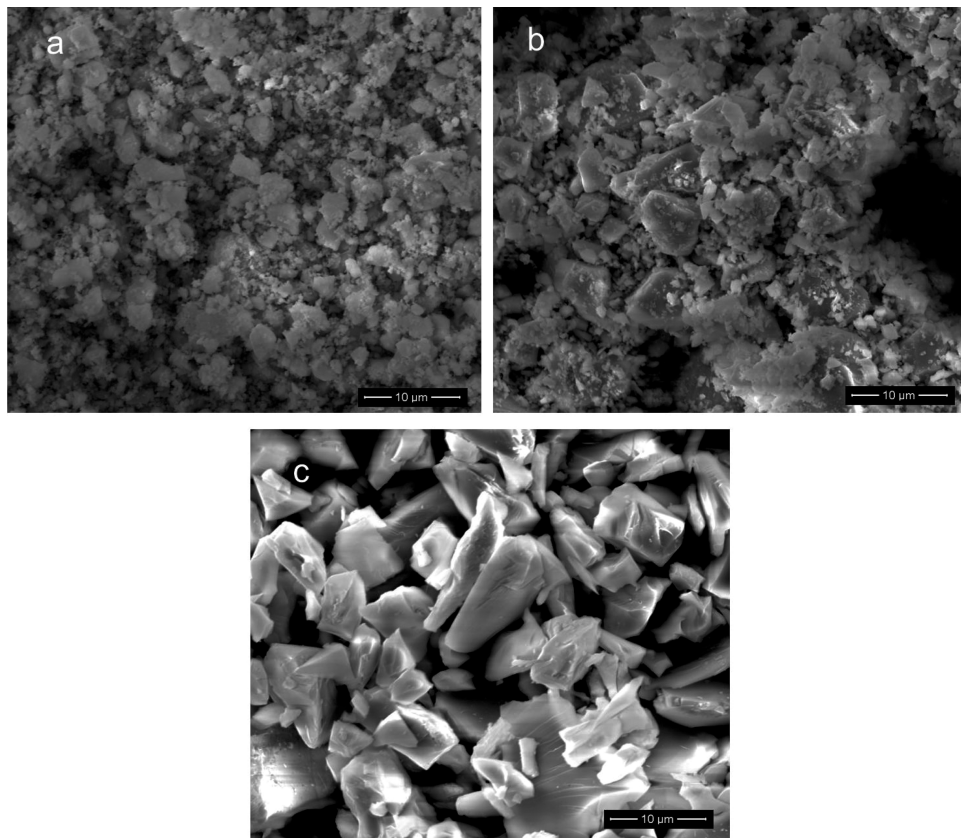


**Figure 2.** SEM images with a 6000 $\times$  magnification of the quartz particles. Quartz I is shown in the top left image (a), quartz II at top right (b), and quartz III below (c). The average surface diameters are 0.5, 1.2, and 4.8  $\mu\text{m}$ .

## RESULTS

In total, the INA of 13 mineral dust samples was investigated with the cryo-microscope (Table 1 and Supporting Information). Figure 1 shows the median freezing temperature,  $T_{50}$ , for each mineral sample. The most active species with  $T_{50}$  values  $>247$  K are quartz I, microcline, ATD, and kaolinite. All other samples

had much lower  $T_{50}$  values ( $<242$  K), but they were still higher than those for pure water, indicating that the nucleation activation barrier was still slightly reduced by the mineral dust particles.

**Untreated Feldspar Samples.** Three different feldspar samples were tested: albite (Na-feldspar), microcline (K-

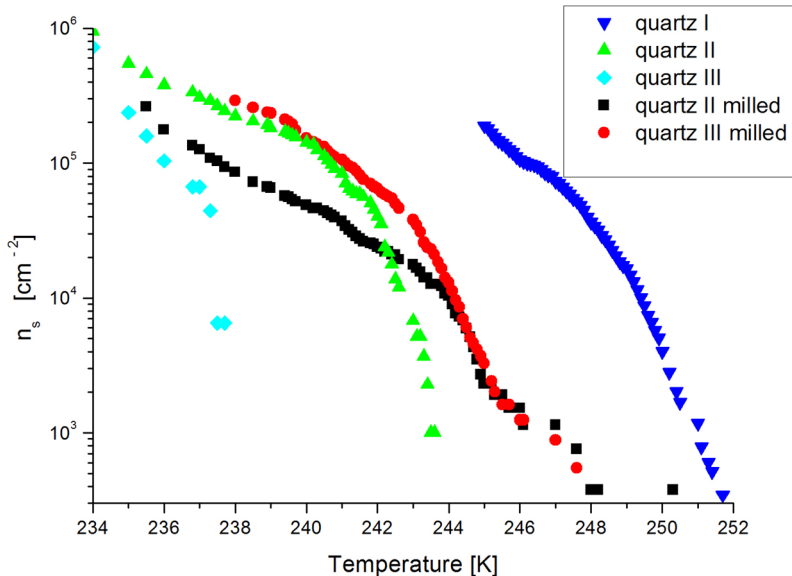


**Figure 3.** Active surface site density depending on temperature plotted for all quartz samples. The  $n_s$  values were obtained using the BET surface values. Quartz I shows the highest surface site density, and the original quartz III sample shows almost no INA. Quartz II and III where milled for 4 min, resulting in a drastic INA increase for quartz III.

feldspar), and andesine (Na/Ca-feldspar). Considerable differences in INA among the feldspars were found: microcline had a  $T_{50}$  value of 249 K, whereas the  $T_{50}$  values for andesine and albite were much lower: 240 and 239 K, respectively. To explain these differences the chemical bulk composition was analyzed with XRD and EDX. Details are given in Table 1. The morphology of albite and microcline was further studied with TEM. The surface structure of microcline is rougher than that of albite, but no significant difference in the morphology of the samples could be identified. The albite sample is crystalline and contains nanosized Pb impurities. These impurities appear on some albite grains, whereas over 70% are highly pure albite. EDX mapping over cracks did not reveal any migration of particular atoms to these sites. Because the penetration depth of X-rays and the exciting electrons is larger than a few hundred nanometers, these analytical methods are not surface specific, and small scale morphological features cannot be discerned. The microcline sample is crystalline and almost pure, except for the above-mentioned albite content. No impurities which may act as IN were found. The atomic composition within the sample does not vary. Macroscopic defects observed in the microcline sample are as common as in albite and can therefore not explain the difference in the INA observed among the feldspars. Furthermore, no organic adsorbates were found with FTIR.

**Untreated Quartz Samples.** The three quartz samples showed significantly different  $T_{50}$  values. The  $T_{50}$  for the most ice active quartz I sample was 249 K. The quartz II and the quartz III samples had  $T_{50}$  values of 239 and 235 K, respectively.

The SEM images of the quartz samples revealed that the quartz I sample (Figure 2a) contained the largest fraction of particles with diameters below 1  $\mu\text{m}$  followed by quartz II and quartz III (Figure 2b,c). The diffractograms of all three tested  $\alpha$ -quartzes show that no other phase was present.

The BET surface area of quartz I sample was 5.5  $\text{m}^2/\text{g}$ . Quartz II had specific BET area of 2.0  $\text{m}^2/\text{g}$  and quartz III 0.5  $\text{m}^2/\text{g}$  (all measured before the initial freezing experiment, i.e., prior to further milling).

**Untreated Other Samples.** Gypsum and calcite became active IN at low temperatures with  $T_{50}$  values of 239 and 237 K,

respectively. The gypsum sample contained around 4% of  $\text{CaSO}_4 \cdot 0.5\text{H}_2\text{O}$ , with the rest being pure  $\text{CaSO}_4 \cdot 2\text{H}_2\text{O}$  (gypsum), given by XRD quantification. Calcite (Sigma-Aldrich) was pure with cube shaped crystals.

Montmorillonite had a  $T_{50}$  of 240 K. A determination of the exact mineral composition is difficult as the layered structure of montmorillonite is not directly observable in powder XRD. By this method only quartz and muscovite were found. The exact quantity of those two components in montmorillonite is unknown, but we expect less than 10% each.

**Untreated Natural Samples.** ATD had the highest  $T_{50}$  (250 K) found in this study. The ATD sample had much smaller particle sizes than the other samples, with hardly any particles larger than 5  $\mu\text{m}$ . Its composition (based on powder XRD phase analysis and SEM-EDX) was 15–20% microcline, 15–20% Na/Ca-feldspar, and 50–60% quartz.  $T_{50}$  was 249 K after heat treatment. The volcanic ash sample contained over 70% albite. Minor components were quartz, other feldspars, titanium iron oxide, and aluminum oxides. The volcanic ash was almost inactive with a  $T_{50}$  of 238 K, but due to the K-feldspar content the initial freezing temperature was much higher (Figure S1, Supporting Information). The natural kaolinite used in this study was no single mineral component sample, as it contained also quartz, muscovite, and halloysite. The average grain size was smaller than for the comparable feldspars. Natural limestone showed the same INA as technical calcite with a  $T_{50}$  of 237 K, and it consisted only of calcite mineral on the basis of the XRD and FTIR analysis.

**Milled Feldspar Samples.** Additional milling of the microcline sample increased the  $T_{50}$  marginally (from 249 to 250 K). Heat treatment of this sample reduces the activity again, leading to the normal median freezing range 249–250 K. For albite, milling had no effect on the  $T_{50}$ , but the initial freezing temperature increased significantly as the albite sample contains some (<1%) K-feldspar and more K-feldspar surface became available during milling.

**Milled Quartz Samples.** Additional milling of both less active quartz samples (quartz II and III) increased their  $T_{50}$  values: after 4 min of milling in the metal swing mill the  $T_{50}$  values

of the samples both changed to 241 K and after 2 min milling time an increase by up to 5 K was visible, whereas the activity of the quartz I sample did not further increase. The initial freezing temperatures of the samples quartz II and III increased from 242 to 246 K, respectively (Figure 3). Heating of the samples after the milling process did not change their INA. The surface areas of both minerals were about  $3 \text{ m}^2/\text{g}$  after milling. The absolute number of active surface nucleation site density  $n_s$  was calculated using the relation given in eq 1, where  $f_{\text{ice}}$  is the frozen fraction at the given temperature  $T$  and  $s$  is the particle surface per droplet obtained directly from BET specific surface area.

$$-n_s(T) = \frac{\log(1 - f_{\text{ice}}(T))}{s} \quad (1)$$

**Temperature-Treated Samples.** Heating the feldspar samples did not change their INA significantly. A slight activity loss was only visible for freshly milled microcline. Nevertheless, within the measurement uncertainty the  $T_{50}$  change only marginally by heat treatments. Temperature treatment of the quartz and the kaolinite samples did not show any significant change in freezing behavior.

**Enzyme-Treated Feldspar Samples.** Except for the particles treated with cellulose onozuka, the freezing curves of microcline changed drastically after enzymatic treatment. The  $T_{50}$  of the enzyme-treated microcline sample shifted to lower temperatures (240 K for microcline and 246 K for fine milled microcline) compared to the pure microcline sample (249 K/250 K) (Table S1, Supporting Information).

After heating the enzyme-treated microcline samples to 773 K, the  $T_{50}$  values returned almost to their initial values ( $T_{50}$  after enzymes and heating: 248 K). The particles mixed with enzymes at low temperatures and direct freezing measurements resulted in the same  $T_{50}$  values as the enzyme-treated samples with incubation.

For albite the same procedure was applied and no distinct loss in INA was observed. In addition, heat and enzyme treatment resulted in no freezing behavior change. The same was observed for andesine.

**Enzyme-Treated Quartz Samples.** A clear loss of INA could be observed for quartz I after the sample was treated with enzymes. Although for treatment with papain the activity was almost unchanged, a treatment with lipase and pronase E clearly shifted the freezing curves to lower temperature values (papain, 249 K; pronase E, 247 K; lipase, 247 K). When all enzymes were applied together,  $T_{50}$  was 244 K. The activity was always restored to the original level after 4 h heating at 773 K.

## ■ DISCUSSION

There is still no molecular description of the exact nature of nucleation sites on mineral dust particles in the literature. Adsorption of water through surface OH groups of the silica is reported,<sup>33</sup> which is in agreement with later studies on kaolinite.<sup>26</sup> Surface amphotericity and size matching between the ice structure and the solid surface has a strong influence on INA. Obviously, it is not the perfect quartz surface itself that nucleates ice at a higher temperature (see the low IN activity of the coarse Quartz III), but rather local defects, which would support the concept of active sites. Those defects may be atomic lattice distortions caused by impurities, leading to a better structure matching between the ice and the particle surface, or crystallographic dislocations. On the basis of the experiments, we suggest that the defect density is different in the three quartz

samples, and that it is increased by mechanical milling, which is known to generate nucleation sites.<sup>34</sup> This would explain the reported variations of INA, which range from quartz with  $T_{50} = 243$  K being the second best IN after the feldspars<sup>24</sup> to studies finding quartz one of the worst IN together with most oxides.<sup>25</sup>

The minerals investigated in this study exhibit median freezing temperature ( $T_{50}$ ) values varying over a range of 13 K between the most (ATD, 250 K) and least (calcite, 237 K) potent IN (Figure 1). Structural analysis showed that there is no direct correlation of the INA with the crystal structure of the minerals. This is especially true for the feldspar group that showed considerable differences in their INA. Milling of the samples increased the INA, which indicates that the freshly produced surfaces provide nucleation active sites that are not accessible otherwise. In particular this is true for the quartz samples. Suppressing INA with specific enzymes with particular chemical functionalities, which can interact with possible surface functional groups on the minerals, was successful in several cases. Subsequent heat treatment to remove the enzymes from the surface resulted in a reactivation of the nucleation activity of the respective mineral.

All these experiments point to the crucial importance of the mineral surface itself and the involvement of the surface chemistry of these particles, as there is no spectroscopic evidence for any particularity to distinguish active surface sites of different quality.

**New Approach—Molecular Sites.** The ice nucleation property of specific quartz samples is not a result of their perfect quartz structure, but rather of local defects acting as nucleation sites. Every site has a certain temperature at which it becomes active. It is still not possible to study these sites directly with conventional methods, but some conclusions can be taken from the immersion freezing experiments carried out in this study. As the silanol groups thought to play an important role in the ice nucleation process<sup>33</sup> are present in almost all silicates that show different  $T_{50}$  values in aqueous immersion, they alone do not act as good IN. Ice nucleation is rather a complex interplay between the forming ice structure and the local surface structure of the mineral particle and therefore the arrangement of the functional groups (on the surface). The local electronic configuration, as well as distance and arrangement of functional groups influence the capability of a particle to act as good IN. Possible functional groups are metal-hydroxyl, fluorine, or ionic oxygen species.<sup>26</sup> The functional groups need to be able to act as a hydrogen bond donor and/or acceptor. A certain particle surface is able to act as IN, if the functional groups are arranged properly. Here, we define a molecular site analogous to (molecular) catalysis as an arrangement of functional groups able to stabilize water molecules in an ice-like structure. A single molecular site may stabilize ice embryos, but to form a good nucleation site, a larger area with domains of molecular sites is needed. These domains nucleate ice at a given temperature, if the stabilized ice cluster is almost as large as the critical ice cluster at this temperature. The molecular sites are of different composition, size, and concentration on different minerals and samples. The assumption of specific molecular sites is based on the fact that with only partial surface coverage with enzymes the INA is lowered, but not totally lost. In addition, the INA of the mineral particles can be increased by increasing the available surface area. The higher INA of quartz I is attributed to an increased concentration of functional groups by the manufacturing (milling) process. For example, quartz III froze almost heterogeneously before milling, whereas introducing further

defects (by milling) increased the activity more than would be expected by just increasing the specific surface area.

Molecular sites are of different form and surface density on mineral dust particles. We assume that the domains of arranged molecular sites conform to a material specific distribution with larger domains, resulting in larger stabilized ice clusters and higher nucleation temperatures being less frequent. With this idea it is possible to explain the increase in nucleation temperatures with increasing surface area.

**Impact of Surface Composition.** The feldspar family has higher  $T_{50}$  values than the quartz sample of comparable surface area in agreement with Atkinson et al.<sup>24</sup> and Yakobi-Hancock et al.<sup>25</sup> for the deposition mode. The structure of feldspars is closely related to quartz, but Si is partly substituted by Al. The  $\text{SiO}_4^{4-}/\text{AlO}_4^{5-}$  tetrahedra in feldspar are slightly tilted due to the charge compensating cations;<sup>35</sup> surface distortions from the basic quartz structure may even be larger and defects (in particular ionic defects) are much more common, so more frequent molecular sites are expected for feldspars.

Nevertheless, the feldspars have quite large differences in  $T_{50}$  values with microcline being active at a much higher temperature in this study and in the study by Atkinson et al.<sup>24</sup> compared to other feldspars. The latest studies<sup>25</sup> showed also good ice nucleation activities in the deposition mode for the orthoclase phase of K-feldspar, so the increased activity of K-feldspar need not be phase specific. The SEM images of the feldspar samples are quite similar and a morphological difference cannot explain the different ice nucleation behavior. On the basis of the TEM-EDX measurements, if ice nucleation occurs at macroscopic defect sites such as cracks, it is not due to a local element accumulation, but rather to the steric configuration there.

Extrinsic INA by organic adsorbates on microcline or its inhibition on the plagioclases can be excluded on the basis of the enzymatic and temperature treatment experiments. The inhibition of ice nucleation sites by enzymes may be understood as steric hindrance or blocking of the site. Further experiments revealed that the loss of INA is a result of a reversible active site hindrance/blocking and not a destruction, as the initial activity was regained after enzyme removal. Our results indicate that the higher INA of the K-feldspar sample is an intrinsic property and not a result of adsorbed organic/biological material. The feldspar surface is richer in defects and distortions compared to quartz. The investigated feldspars have different counter cations with different ionic radii ( $r_{\text{K}^+} > r_{\text{Na}^+} \sim r_{\text{Ca}^{2+}}$ ).<sup>36</sup> In addition the plagioclases (Na/Ca-feldspars) have a higher Al/Si ordering than the K-feldspars.

The measurements leave only the conclusion that the difference in the INA of the feldspars is a result of the difference in ionic radius of the cations and therefore the local chemical configuration at the surface. The surface cations released into the surface bilayer may interact with water to enhance/inhibit ice formation. The resulting depletion of cations in the outermost layer<sup>36</sup> may be different for each cation due to the differences in ionic radii. The ion charge density of the cations of the mineral was already suggested to influence ice nucleation on mineral surfaces.<sup>28</sup> The cations around the surface have different affinity to water molecules and potential bonds are of different strength. Surface calcium ions on calcite are known to bind the water quite tightly and thus inhibit ice nucleation by fixing the water molecules in ice structure mismatching locations.<sup>37</sup> The difference in INA of microcline and the plagioclases may also be a result of the more random cation/aluminum distribution in the K-feldspars compared to the Na/Ca feldspars.

As already mentioned, feldspar surfaces are cation deficient in aqueous solution. The tendency of the surface to interact with water molecules is increased by this process as dangling bonds remain at the surface. The ions in the surface bilayer are hydrated by the water matrix. The hydration shells of  $\text{Ca}^{2+}$ ,  $\text{Na}^+$ , and  $\text{K}^+$  ions have different sizes and shapes.  $\text{Ca}^{2+}$  and  $\text{Na}^+$  belong to the chaotrope family (structure breaking ions) whereas  $\text{K}^+$  is a kosmotrope (structure making ion).<sup>38,39</sup> Small ions with high charge density are considered to be chaotrope and have a strong interaction with water. The weaker water–water hydrogen bonds are broken to form the hydration shells with larger residence times of water molecules compared to the shells of kosmotropic ions. These strong chaotrope–water interactions inhibit an ice-like structuring of water molecules in the vicinity of the ions. Kosmotropes like  $\text{K}^+$  on the other hand have a weaker interaction with water than the intermolecular water–water interaction. The  $\text{K}^+$  ions form hydration shells, but the water molecules are bonded more weakly and have high exchange rates. Therefore, any thermodynamic phase change of water by  $\text{K}^+$  ions is kinetically less hindered than by chaotrope ions.

In feldspar the cations released into the water stay close to the surface due to surface charging and charge compensation and are then able to interact with water molecules. In the case of  $\text{Ca}^{2+}$  and  $\text{Na}^+$ , ice nucleation is inhibited by their chaotropic behavior, whereas  $\text{K}^+$  has a positive or at least a neutral effect. In addition, it was shown that KOH is easily incorporated into the ice structure.<sup>40,41</sup> The size of  $\text{K}^+$  is around the size of a  $\text{H}_3\text{O}^+$  ion, whereas  $\text{Na}^+$  and  $\text{Ca}^{2+}$  are far too small to fit well into the ice structure. This would further lower the negative effect of the  $\text{K}^+$  ions to the formation of ice-like structures close to the vicinity of the surface bilayer. This is in agreement with a former study<sup>28</sup> where lower ice nucleation temperatures were found for micas containing  $\text{Al}^{3+}$  ions instead of  $\text{K}^+$  ions, where again the aluminum ion has a much higher charge density.

**Situation for Other Minerals.** Our kaolinite sample contains small amounts of K-feldspar, which gives the sample most of its INA together with a slightly larger surface area. Any exact explanation of the ice nucleation behavior of our montmorillonite sample is difficult, as exact mineral composition analysis and structure determination are lacking. A distinct phase identification by XRD was not possible due to the layered stacking structure of montmorillonite. On the basis of the SEM-EDX, the larger amounts of  $\text{Mg}^{2+}$  compared to  $\text{K}^+$ ,  $\text{Na}^+$ , and  $\text{Ca}^{2+}$  found suggest chaotropic influence of the magnesium ions if the surfaces of the mineral support ice-like arranged water molecules. Nevertheless, the montmorillonite acts as a heterogeneous IN, but at rather low temperatures compared to K-feldspar.

Neither calcite nor gypsum show high  $T_{50}$  values. As already reported, the calcite surface has a strong affinity to water molecules.<sup>37</sup> The water molecules are tightly bound to the surface and cannot arrange in ice-like structures. The water molecules are possibly bound to hydrolysis species, chemisorbed on the surface of calcite.<sup>42</sup> In gypsum, the strong calcium–water interaction may lead to a similar behavior.

In agreement with the feldspars, the investigated volcanic ash acts as a rather poor IN with a  $T_{50}$  of 238 K. The ash sample from the Eyjafjallajökull eruption 2010 is mainly composed of the weak IN albite (Na-feldspar). The higher initial freezing temperature can be easily explained by the inhomogeneity of the sample. The titanium–iron oxide which was found in the ash seems to have no influence on the INA, but no experiments on single minerals could be performed. This partly explains why in a former study volcanic ash showed both high IN activity, as well as almost

none.<sup>23</sup> The difference in the ash composition may explain the different results. K-feldspar rich volcanic ash has a larger tendency to act as a good IN than ash containing mainly plagioclases (Na/Ca-feldspar). It cannot be stated directly that only the mineral composition determines the INA as volcanic ash eruptions are often accompanied by sulfuric acid and other gases that may alter the surface and ice nucleation properties.<sup>43</sup>

The ATD sample had a slightly larger surface area than the other dust samples, probably leading to a slightly overestimated  $T_{50}$  value compared to the other samples. Still, the ATD sample was a rather good IN, which was not surprising due to its K-feldspar content. In addition, the quartz content may also act as IN, depending on the preprocessing of the sample.

## CONCLUSION

Mineral dusts are known to be active IN. In this study, the ice nucleation behavior of various mineral samples was investigated with a special focus on feldspars, which are known to be among the most ice nucleation active species.<sup>24</sup>

The feldspars are more ice nucleation active than most quartz samples, and K-feldspar is by far the most active IN of the feldspar family. The size of the cation, and its binding energy toward water are the key factors determining INA.

Different quartz samples showed a large discrepancy of their INA. With the presented idea of domains of molecular sites able to bind and arrange water molecules in an ice-like structure acting as ice nucleation sites, we suggest that the history of the quartz particles and dust particles in general has an important influence. INA is enhanced by introducing more defects to a quartz surface by mechanical milling. The nucleation sites suggested here are not necessarily the same on each particle, but rather caused by a stochastic arrangement of functional groups which are able to bind water molecules. Therefore, nucleation site sizes, as well as the corresponding nucleation temperature, conform to a statistical distribution. Consequently, the freezing curves determined with our experimental setup can be shifted to higher temperatures by increasing the particle surface for active IN like K-feldspar. Still, an open task for future work will be to understand the processes that lead to site formation on the molecular level.

## ASSOCIATED CONTENT

### Supporting Information

The Supporting Information includes a table with all measured freezing temperatures and particle sizes, freezing spectra given as active surface site density ( $n_s$ ), and a freezing spectrum of single measurement runs. This material is available free of charge via the Internet at <http://pubs.acs.org>.

## AUTHOR INFORMATION

### Corresponding Author

\*Hinrich Grothe. E-mail address: grothe@tuwien.ac.at. Telephone number: +43 (1) 58801 165122.

### Present Addresses

<sup>II</sup>University of Toronto, Chemistry Department, St. George St. 80, ON M5S 3H6 Toronto, Canada.

<sup>†</sup>Max-Planck-Institute for Chemistry, Dept. Multiphase Chemistry, Hahn-Meitner-Weg 1, 55128 Mainz, Germany.

### Notes

The authors declare no competing financial interest.

## ACKNOWLEDGMENTS

We thank the Austrian Science Fund (FWF) for the financial support (Project number P23027 and P26040). Electron microscopy and X-ray diffraction was carried out using facilities at the University Service Centre for Transmission Electron Microscopy (USTEM) and X-ray diffraction (XRC), Vienna University of Technology, Austria.

## REFERENCES

- (1) Solomon, S.; Qin, D.; Manning, M.; Chen, Z.; Marquis, M.; Averyt, K. B.; Tignor, M.; Miller, H. L. *IPCC, 2007: Climate Change 2007: The Physical Science Basis. Contribution of Working Group I to the Fourth Assessment Report of the Intergovernmental Panel on Climate Change*; Cambridge University Press: Cambridge, U.K. and New York, 2007.
- (2) Baker, M. B.; Peter, T. Small-Scale Cloud Processes and Climate. *Nature* **2008**, *451*, 299–300.
- (3) Baker, J. M.; Dore, J. C.; Behrens, P. Nucleation of Ice in Confined Geometry. *J. Phys. Chem. B* **1997**, *101*, 6226–6229.
- (4) Lohmann, U. A Glaciation Indirect Aerosol Effect Caused by Soot Aerosols. *Geophys. Res. Lett.* **2002**, *29*, 11.
- (5) DeMott, P. J.; Prenni, A. J.; Liu, X.; Petters, M. D.; Twohy, C. H.; Richardson, M. S.; Eidhammer, T.; Kreidenweis, S. M.; Rogers, D. C. Predicting Global Atmospheric Ice Nuclei Distributions and their Impacts on Climate. *Proc. Natl. Acad. Sci.* **2010**, *107*, 11217–11222.
- (6) Pruppacher, H. R.; Klett, G. D. *Microphysics of Clouds and Precipitation*; Kluwer Academic Publishers: Amsterdam, 1997.
- (7) Kärcher, B.; Spichtinger, P. Cloud-Controlling Factors of Cirrus Clouds in the Perturbed Climate System: Their Relationship to Energy Balance, Atmospheric Dynamics, and Precipitation, *Strüngmann Forum Reports* **2009**, *2*.
- (8) Hoose, C.; Möhler, O. Heterogeneous Ice Nucleation on Atmospheric Aerosols: a Review of Results from Laboratory Experiments. *Atmos. Chem. Phys.* **2012**, *12*, 9817–9854.
- (9) Murray, B. J.; O'Sullivan, D.; Atkinson, J. D.; Webb, M. E. Ice Nucleation by Particles Immersed in Supercooled Cloud Droplets. *Chem. Soc. Rev.* **2012**, *41*, 6519–54.
- (10) Kumai, M. Snow Crystals and the Identification of the Nuclei in the Northern United States of America. *J. Meteorol.* **1961**, *18*, 139–150.
- (11) Isono, B. K.; Ikebe, Y. On the Ice-Nucleating Ability of Rock-Forming Minerals and Soil Particles. *J. Meteorol. Soc. Jpn.* **1960**, *38*, 213–230.
- (12) Wiacek, A.; Peter, T.; Lohmann, U. The Potential Influence of Asian and African Mineral Dust on Ice, Mixed-Phase and Liquid Water Clouds. *Atmos. Chem. Phys.* **2010**, *10*, 8649–8667.
- (13) Pratt, K. A.; DeMott, P. J.; French, J. R.; Wang, Z.; Westphal, D. L.; Heymsfield, A. J.; Twohy, C. H.; Prenni, A. J.; Prather, K. A. In Situ Detection of Biological Particles in Cloud Ice-Crystals. *Nat. Geosci.* **2009**, *2*, 398–401.
- (14) Cziczo, D. J.; Froyd, K. D.; Hoose, C.; Jensen, E. J.; Diao, M.; Zondlo, M. A.; Smith, J. B.; Twohy, C. H.; Murphy, D. M. Clarifying the Dominant Sources and Mechanisms of Cirrus Cloud Formation. *Science* **2013**, *340*, 1320–1324.
- (15) Lüönd, F.; Stetzer, O.; Welti, A.; Lohmann, U. Experimental Study on the Ice Nucleation Ability of Size-Selected Kaolinite Particles in the Immersion Mode. *J. Geophys. Res.* **2010**, *115*, 27.
- (16) Murray, B. J.; Broadley, S. L.; Wilson, T. W.; Atkinson, J. D.; Wills, R. H. Heterogeneous Freezing of Water Droplets Containing Kaolinite Particles. *Atmos. Chem. Phys.* **2011**, *11*, 4191–4207.
- (17) Pinti, V.; Marcolla, C.; Zobrist, B.; Hoyle, C. R.; Peter, T. Ice Nucleation Efficiency of Clay Minerals in the Immersion Mode. *Atmos. Chem. Phys.* **2012**, *12*, 5859–5878.
- (18) Welti, A.; Lüönd, F.; Kanji, Z. A.; Stetzer, O.; Lohmann, U. Time Dependence of Immersion Freezing. *Atmos. Chem. Phys. Discuss.* **2012**, *12*, 12623–12662.
- (19) Zimmermann, F.; Weinbruch, S.; Schütz, L.; Hofmann, H.; Ebert, M.; Kandler, K.; Worringen, A. Ice Nucleation Properties of the most Abundant Mineral Dust Phases. *J. Geophys. Res.* **2008**, *113*, D23204.

- (20) Eastwood, M. L.; Cremel, S.; Gehrke, C.; Girard, E.; Bertram, A. K. Ice Nucleation on Mineral Dust Particles: Onset Conditions, Nucleation Rates and Contact Angles. *J. Geophys. Res.* **2008**, *113*, D22203.
- (21) Connolly, P. J.; Möhler, O.; Field, P. R.; Saathoff, H.; Burgess, R.; Choularton, T.; Gallagher, M. Studies of Heterogeneous Freezing by Three Different Desert Dust Samples. *Atmos. Chem. Phys.* **2009**, *9*, 2805–2824.
- (22) Steinke, I.; Möhler, O.; Kiselev, A.; Niemand, M.; Saathoff, H.; Schnaiter, M.; Skrotzki, J.; Hoose, C.; Leisner, T. Ice Nucleation Properties of Fine Ash Particles from the Eyjafjallajökull Eruption in April 2010. *Atmos. Chem. Phys.* **2011**, *11*, 12945–12958.
- (23) Hoyle, C. R.; Pinti, V.; Welti, A.; Zobrist, B.; Marcolli, C.; Luo, B.; Höskuldsson, Á.; Mattsson, H. B.; Stetzer, O.; Thorsteinsson, T.; Larsen, G.; Peter, T. Ice Nucleation Properties of Volcanic Ash from Eyjafjallajökull. *Atmos. Chem. Phys.* **2011**, *11*, 9911–9926.
- (24) Atkinson, J. D.; Murray, B. J.; Woodhouse, M. T.; Whale, T. F.; Baustian, K. J.; Carslaw, K. S.; Dobbie, S.; O'Sullivan, D.; Malkin, T. L. The Importance of Feldspar for Ice Nucleation by Mineral Dust in Mixed-Phase Clouds. *Nature* **2013**, *498*, 355–358.
- (25) Yakobi-Hancock, J. D.; Ladino, L. A.; Abbatt, J. P. D. Feldspar Minerals as Efficient Deposition Ice Nuclei. *Atmos. Chem. Phys.* **2013**, *13*, 11175–11185.
- (26) Hu, X. L.; Michaelides, A. Ice Formation on Kaolinite: Lattice Match or Amphoterism? *Surf. Sci.* **2007**, *601*, 5378–5381.
- (27) Hu, X. L.; Michaelides, A. The Kaolinite (001) Polar Basal Plane. *Surf. Sci.* **2010**, *604*, 111–117.
- (28) Shen, J. H.; Klier, K.; Zettlemoyer, A. C. Ice Nucleation by Micas. *J. Atmos. Sci.* **1977**, *34*, 957–960.
- (29) Pummer, B. G.; Bauer, H.; Bernardi, J.; Bleicher, S.; Grothe, H. Suspendable Macromolecules are Responsible for Ice Nucleation Activity of Birch and Conifer Pollen. *Atmos. Chem. Phys.* **2012**, *12*, 2541–2550.
- (30) ICDD, PDF-4 2013 (Database); International Centre for Diffraction Data: Newtown Square, PA, USA, 2013.
- (31) Weast, C. R.; Astle, M. J. *CRC Handbook of Chemistry*; CRC Press: Boca Raton, FL, 1981.
- (32) Conen, F.; Henne, S.; Morris, C. E.; Alewell, C. Atmospheric Ice Nucleators Active  $\geq -12^{\circ}\text{C}$  Can be Quantified on PM10 Filters. *Atmos. Meas. Technol.* **2012**, *5*, 321–327.
- (33) Klier, K.; Shen, J. H.; Zettlemoyer, A. C. Water on Silica and Silicate Surfaces. I. Partially Hydrophobic Silicas. *J. Phys. Chem.* **1973**, *77*, 1458–1465.
- (34) Hiranuma, N.; Hoffmann, N.; Kiselev, A.; Dreyer, A.; Zhang, K.; Kulkarni, G.; Koop, T.; Möhler, O. Influence of Surface Morphology on the Immersion Mode Ice Nucleation Efficiency of Hematite Particles. *Atmos. Chem. Phys.* **2014**, *14*, 2315–2324.
- (35) Hons, G. L. Behavior of Alkali Feldspars: Crystallographic Properties and Characterization of Composition and Al-Si Distribution. *Am. Mineral.* **1986**, *71*, 869–890.
- (36) Fenter, P.; Teng, H.; Geissbühler, P.; Hanchar, J.; Nagy, K.; Sturchio, N. Atomic Scale Structure of the Orthoclase (001)–Water Interface Measured with High Resolution X-Ray Reflectivity. *Geochim. Cosmochim. Acta* **2000**, *64*, 3663–3673.
- (37) Lardge, J. S.; Duffy, D. M.; Gillan, M. J.; Watkins, M. Ab Initio Simulations of the Interaction between Water and Defects on the Calcite {1014} Surface. *J. Phys. Chem. C* **2010**, *114*, 2664–2668.
- (38) Yizhak, M. Effect of Ions on the Structure of Water: Structure Making and Breaking. *Chem. Rev.* **2009**, *109*, 1346–1370.
- (39) Zangi, R. Can Salting-In/Salting-Out Ions be Classified as Chaotropes/Kosmotropes? *J. Phys. Chem. B* **2010**, *114*, 643–650.
- (40) Salzmann, C. G.; Radaelli, P. G.; Hallbrucker, A.; Mayer, E.; Finney, J. L. The Preparation and Structures of Hydrogen Ordered Phases of Ice. *Science* **2006**, *311*, 1758–1761.
- (41) Tajima, Y.; Matsu, T.; Suga, H. Phase Transition in KOH-Doped Hexagonal Ice. *Nature* **1982**, *299*, 810–812.
- (42) Stipp, S. L. L. Toward a Conceptual Model of the Calcite Surface: Hydration, Hydrolysis, and Surface Potential. *Geochim. Cosmochim. Acta* **1999**, *63*, 3121–3131.
- (43) Augustin-Bauditz, S.; Wex, H.; Kanter, S.; Ebert, M.; Niedermeier, D.; Stolz, F.; Prager, A.; Stratmann, F. The immersion mode ice nucleation behavior of mineral dusts: A comparison of different pure and surface modified dusts. *Geophys. Res. Lett.* **2014**, *41*, 7375–7382.